Membrane Mediated Interactions between Peptides. 2. Many-Body Effects

G.V. Miloshevsky, M.B. Partenskii, P.C. Jordan

Department of Chemistry, Brandeis University, Waltham, MA 02454, USA

Abstract

We study the elastic energy $F(s,d)$ for clusters of n inclusions inserted into a membrane and contrast cases with n inclusions arranged in an equilateral polygon, and with m (either 0 or 1) inclusions in the center, denoted (n,m). Minimized with respect to the contact slope s (the gradient of the deformation profile at the membrane-inclusion interface), the two-body interaction free energy $F_{min}(d)$ is repulsive for all inter-inclusion distances d. However, with increasing numbers of inclusions interaction may become attractive, implying significant many-body effects. Calculations are performed for DMPC and GMO membranes.

For the $(4,1)$ cluster F_{min} is repulsive for all d, however the energy profile is flattened at short separations compared to the two inclusions case. For the $(5,0)$ case F_{min} is slightly attractive at short distances. The $(6,1)$ cluster forms a stable aggregate with distinct attractive and repulsive regions. The energy profile is similar to earlier predictions for two-dimensional hexagonal lattices.

As in the two-body case, the $F(s,d)$ behaviour changes if the slope s is fixed. Again, at small $|s| \sim 0$ interaction is attractive, while at large negative slopes, it is repulsive. In the intermediate region the free energy is a sigmoidal function of d. In agreement with previous results, at higher concentrations (seven inclusions, small d) the equilibrium slope, s_{min}, shifts towards $s \sim 0$. However, in no way does this argue for fixing $s \sim 0$ for a single (isolated) inclusion. Finally, we consider how clustering can affect the lifetime of ion channels.

Euler-Lagrange Equation and Boundary Conditions

The elastic problem described in [1] is solved in the uniform approximation leading to an Euler-Lagrange equation for $u(x,y)$

$$b\,\Delta^2 u(x,y) + a\,u(x,y) = 0 \qquad (1)$$

with

$$a = 2B/h_0, \qquad b = h_0 K/2.$$

B and K are stretching and bending constants, more generally r-dependant; h_0 is the unperturbed hydrophobic membrane thickness. The boundary conditions at the edge of the computational domain are those of Eq. 3 of the neighbouring poster [1]. At the internal boundaries, L, $u(\mathrm{r})$ is fixed at u_0 and the contact slope s is assumed isotropic. Thus

$$u(\mathrm{r}_L) = u_0, \qquad \nabla u(\mathrm{r}_L) = s \qquad (2)$$

Sometimes, we minimize the free energy, $\boldsymbol{F}$, with respect to s, yielding $\boldsymbol{F}_{min}$, at

$$s = s_{min} \qquad (3)$$

The solution algorithm for this elastic problem is described in [1]. Here we use elastic parameters representative of gramicidin A (GA) inserted into DMPC membranes: hydrophobic mismatch, $u_0 = 1.65\,\text{Å}$, inclusion radius, $r_0 = 10\,\text{Å}$.

Model and Computational Details

The model and boundary conditions used here are those described in our poster [1]. The new computations illustrate behavior in a DMPC membrane containing the embedded clusters *(n,m)*, with *n* the number of inclusions arranged in the regular equilateral polygon and *m* the inclusion at the cluster origin. We consider the following cases: n=3, 4, 5, 6, 6-1 (6-1 indicates occupancy of only 5 of the 6 inclusion sites) and m=0, 1.

Figure 1 is a schematic view of the computational domain for the (*5,1*) cluster. The distance *d* is measured between the cluster's center and the edges of lateral inclusions. Protein radii are 10 Å. Two layers of grid points are used for the boundary conditions at the edges of both the computational domain and each inclusion. At the external edge of the system the boundary condition $u=0$ is applied. At inclusion edges the fixed value $u_0 = 1.65$ Å is used. The boundary slope *s* is azimuthally symmetrical along each boundary circle. The distortion field is computed at the interior points.

Many-body effects in membrane-mediated interactions

Figures 2–4 illustrate the deformation free energy as a function of the boundary slope s for a range of distances d. The profiles are parabolic; the minimum energy corresponds to the contact slope s_{min}. *(3,1), (4,1)* and *(6,1)* clusters are shown. For *(3,1)* and *(4,1)* clusters interaction is repulsive, but for the *(4,1)* cluster (**Figure 3**) the minimum energy profile is very smooth in the range of distances from 11 to 20 Å. Starting with *(5,0)* and *(5,1)* clusters, an attractive branch develops at small d. The attractive well is fully developed for the *(6,1)* cluster (**Figure 4**).

Figure 5 shows deformational free energy profiles, $F(d)$, for a *(6,1)* cluster for a range of cylindrically symmetrical contact slopes s ($-0.1 \le s \le 0.1$). As with two inclusions, van der Waals type behavior is found for both $s>0$ and $s<0$ [1]. The curve corresponding to the optimal (energy minimized) slope is also shown, $s_{min} \to 0$ for small d.

Figures 6 & 7 present deformation energy profiles, $F(d)$, for *(n,0)* and *(n,1)* clusters for the contact slopes $s=s_{min}$ (**Figure 6**) and $s=0$ (**Figure 7**). With $s=0$ the energy is strongly attractive for all clusters. In general, the energy of *(n,1)* clusters with $s=0$ is less than that of *(n,0)* clusters. At smaller d, however, *(n,1)* clusters with $n>5$ are energetically favored over *(n,0)* clusters. Here an attractive region appears at $d < 20$ Å, separated by a barrier from the repulsive region for both $m=0$ and $m=1$ clusters. Attraction is still found for a *(6-1,1)* cluster with a lateral vacancy (not shown). However, the *(6-1,0)* cluster is unstable (also not shown).

Many-body influences on a channel's effective spring constant

Nielsen et al. proposed [4] a "linear spring model" describing the inclusion-induced deformation energy F_{def}:

$$F_{def}(u_0) = H(2u_0)^2 \qquad (4)$$

where H is an effective Hooke's Law spring constant. This proved to be a very convenient way of describing membrane influences on channel lifetimes. Eq. 4 is exact for an individual inclusion if either condition $s=s_{min}$, or $s=0$ is used.

We now consider how inter-inclusion interaction affects this effective spring constant by considering the deformational energy change in response to a small variation δu_0 of u_0 for one channel in a cluster, keeping u_0 fixed for all other inclusions. Then, H can be expressed in terms of the variation of the free energy δF_{def} as

$$H = \delta F_{def} / (4\, \delta u_0\, u_0) \qquad (5)$$

We consider a *(6,1)* cluster and first test the approximation, Eq. 4. Results for the central channel and a lateral one are presented in **Figure 8**. The Hooke's law model, Eq. 4, is quite a good approximation for $d > 30$ Å for the central inclusion and for $d > 25$ Å for a lateral one. In this range Eq. 5 is also a reasonable approximation. The results presented in **Figure 9** show that H drops sharply as d decreases, which implies that clustering can significantly increase ion channel lifetimes (assuming that the choice, $s=0$, is correct).

The results of **Figure 8** for the central inclusion are interesting on their own. They show that the stretching energy is linear in δu_0 at large d and quadratic for small d. This is further indication of strong stabilization of the channel due to clustering. At small d, membrane thinning due to lateral inclusions makes the central channel practically unstretched. Consequently, Eqs. 4 and 5 must be replaced by

$$F_{def}(u_0) = H(2\,\delta u_0)^2 \qquad (4')$$

In other words, for the central channel the dimer becomes more stable than the monomers! This cluster induced stabilization is less significant for lateral channels.

Conclusions

- For relaxed boundary conditions, an attractive region appears at $d < 20$ Å for the *(5,0)* cluster, and becomes more prominent as the number of inclusions increases. For constrained slopes, $s=0$, increasing n and m makes the (attractive) energy profile steeper.
- For constrained slopes, $s=0$, clusters containing a central inclusion are favored in energy compared to those with no central inclusion. For optimal contact slopes, s_{min}, the clusters with high n and $m=1$ are energetically favorable at distances $d < 20$ Å.
- The free energy profiles exhibit van der Waals type behavior for both $s<0$ and $s>0$.
- The optimal contact slope, $s_{min} \rightarrow 0$, at small d for clusters with large n and with $m=1$.
- Deformation free energies were calculated assuming cylindrically symmetrical slopes. The results presented in [1] show that accounting for slope anisotropy makes interaction more attractive for all clusters. In addition, clusters with $n<5$ treated with the relaxed anisotropic boundary conditions may well become stable at small d.
- The effective elastic constant and the GA channel lifetime can be strongly affected by many-body interactions. Results are dependent on the position of the channel in the cluster and on the distance d. For $s=0$, all channels become more stable as d decreases. For the central channel in the dense *(6,1)* cluster, the conducting (dimeric) state is more stable than the separated two monomer state.

References

1. M. B. Partenskii, G. V. Miloshevsky & P.C. Jordan, *Biophysical Society Meeting* 2002, Poster 716

2. P. C. Jordan, G. V. Miloshevsky & M. B. Partenskii, In "Interfacial Catalysis," G. Volkov ed., Marcel Dekker, 2002 (in press)

3. Dan N. et al, *J. Phys. II (France),* **4**:1713-1725

4. C. Nielsen, M. Goulian & O. S. Andersen, *Biophys. J.* **74**:1966-1983, 1998.

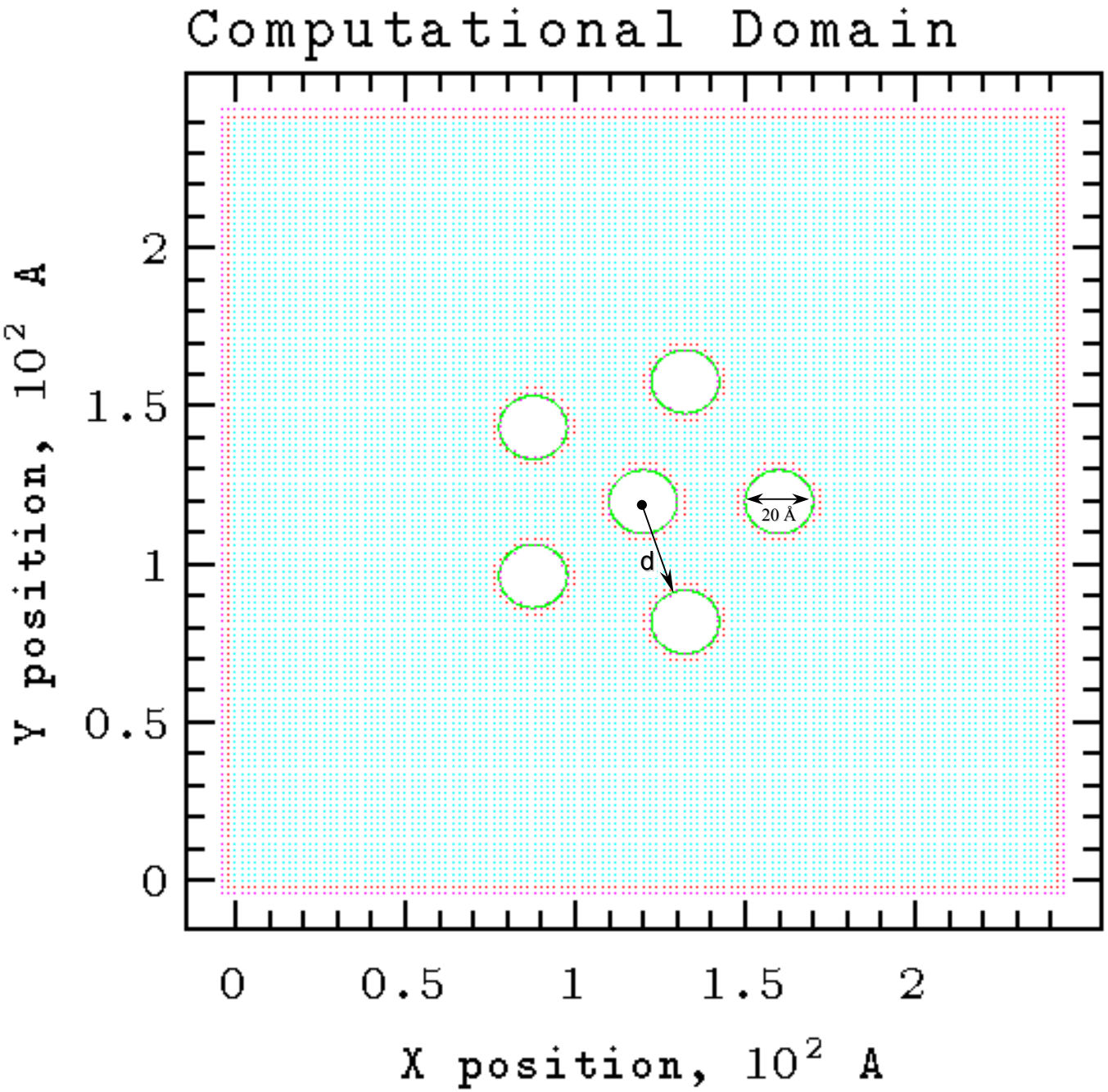

Fig. 1 Illustration of the protein aggregate (n,m) with n=5 and m=1. The distance d is measured from the cluster origin. Grid points in cyan color are the interior points at which the deformation field is computed. Red and magenta points are two layers of points for boundary conditions at the edges of both the total computational domain and each inclusion.

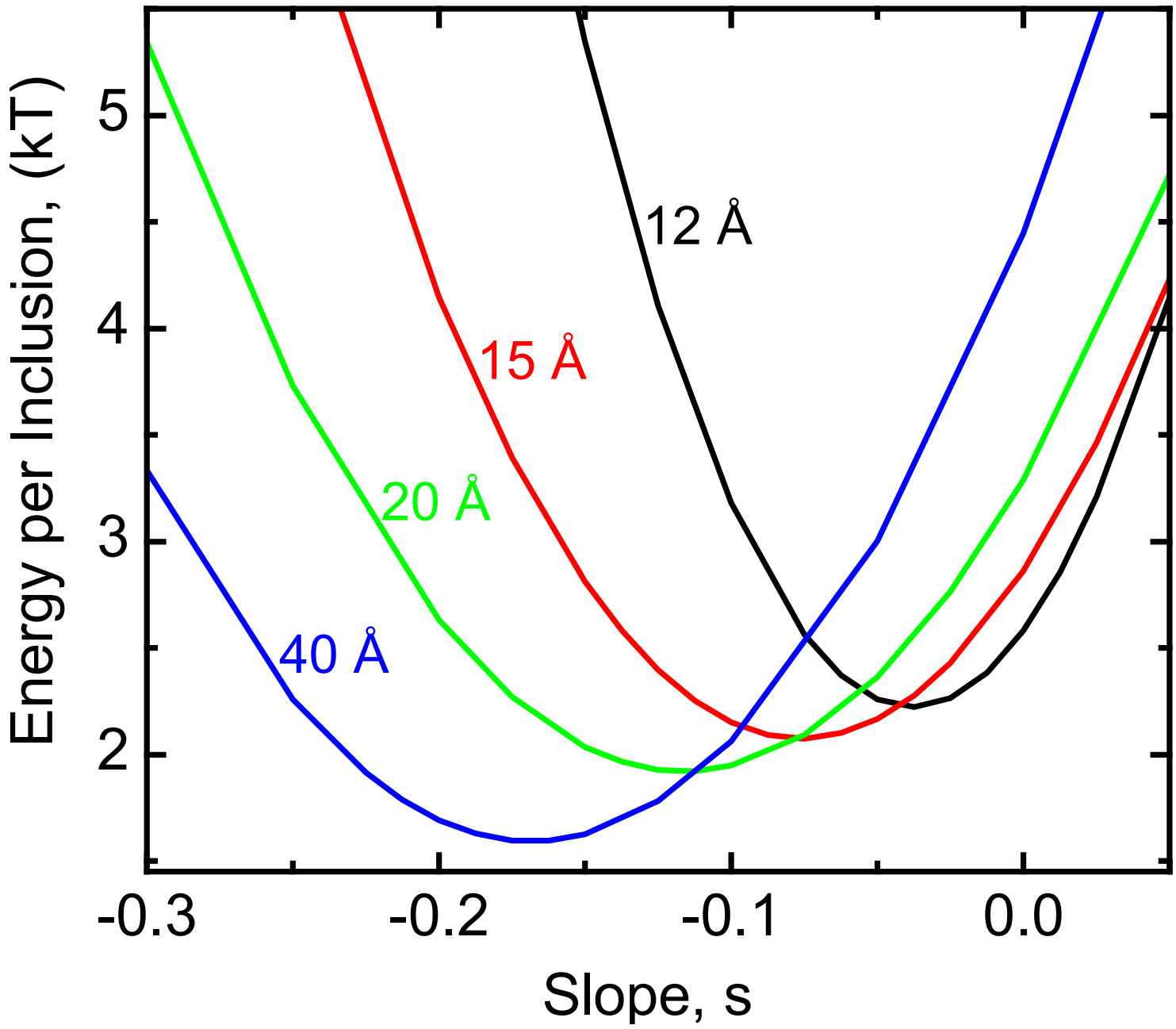

Fig. 2 Deformation free energy per inclusion for the (3,1) cluster as a function of the contact slope, s. Free energy profiles are shown for different interinclusion distances, d.

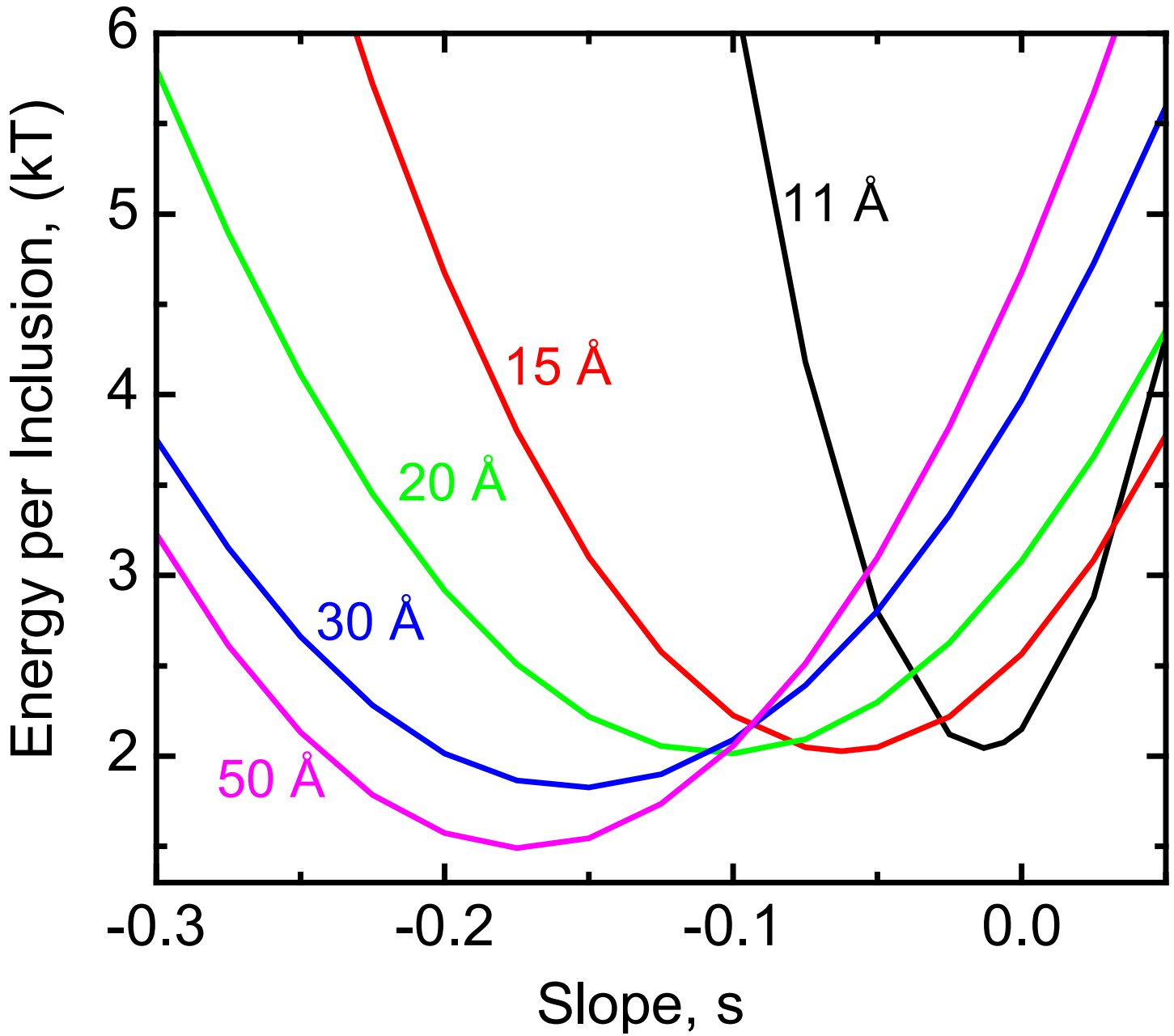

Fig. 3 Deformation free energy per inclusion for the (4,1) cluster as a function of the contact slope, s. Free energy profiles are shown for different interinclusion distances, d.

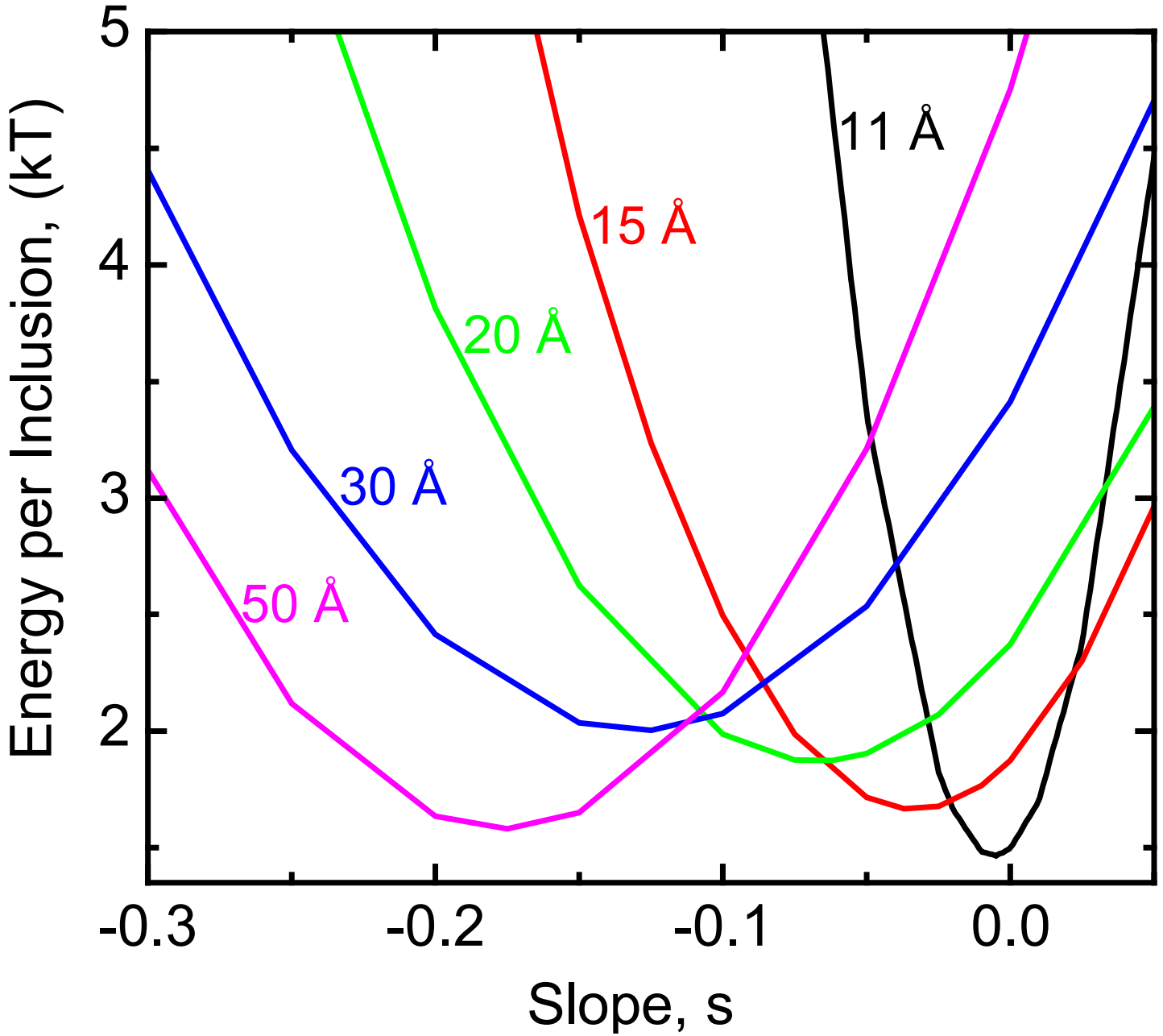

Fig. 4 Deformation free energy per inclusion for the (6,1) cluster as a function of the contact slope, s. Free energy profiles are shown for different interinclusion distances, d.

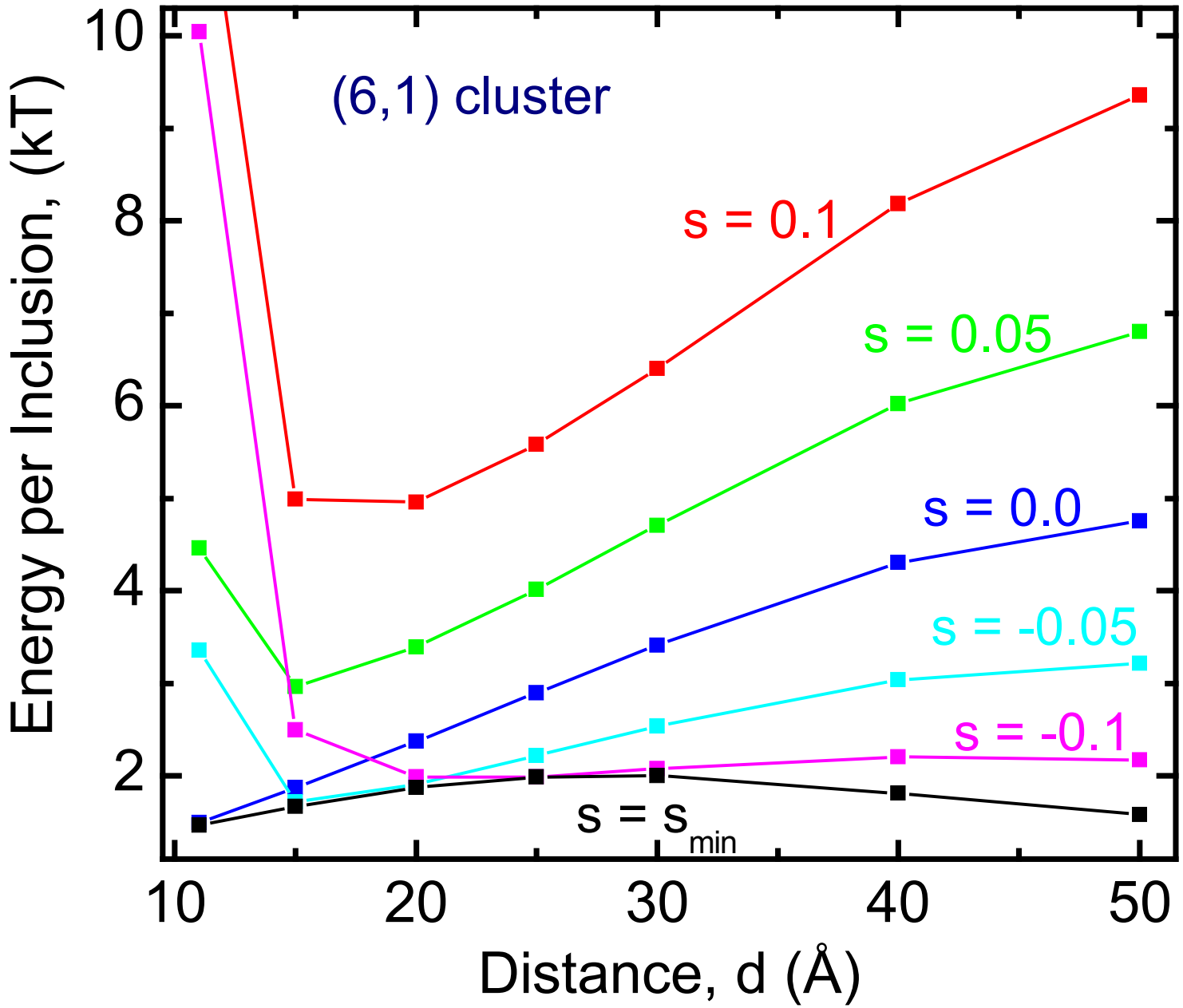

Fig. 5 Deformation free energy per inclusion for the (6,1) cluster as a function of the distance, d, for various contact slopes, s.

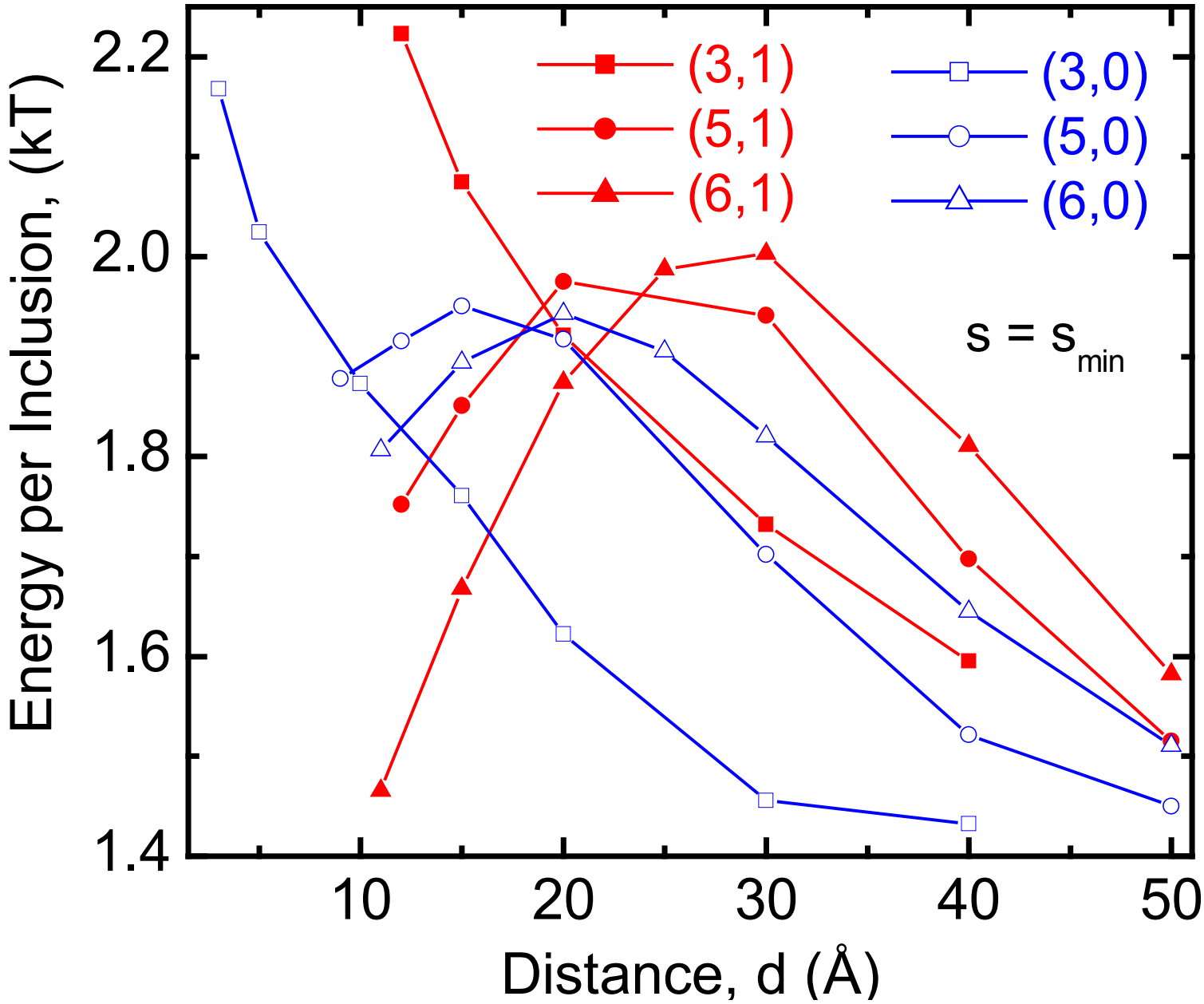

Fig. 6 Free energy of membrane deformation per inclusion as a function of distance, d, for $s=s_{min}$. Results are compared for clusters with (m=1) and without (m=0) a central inclusion.

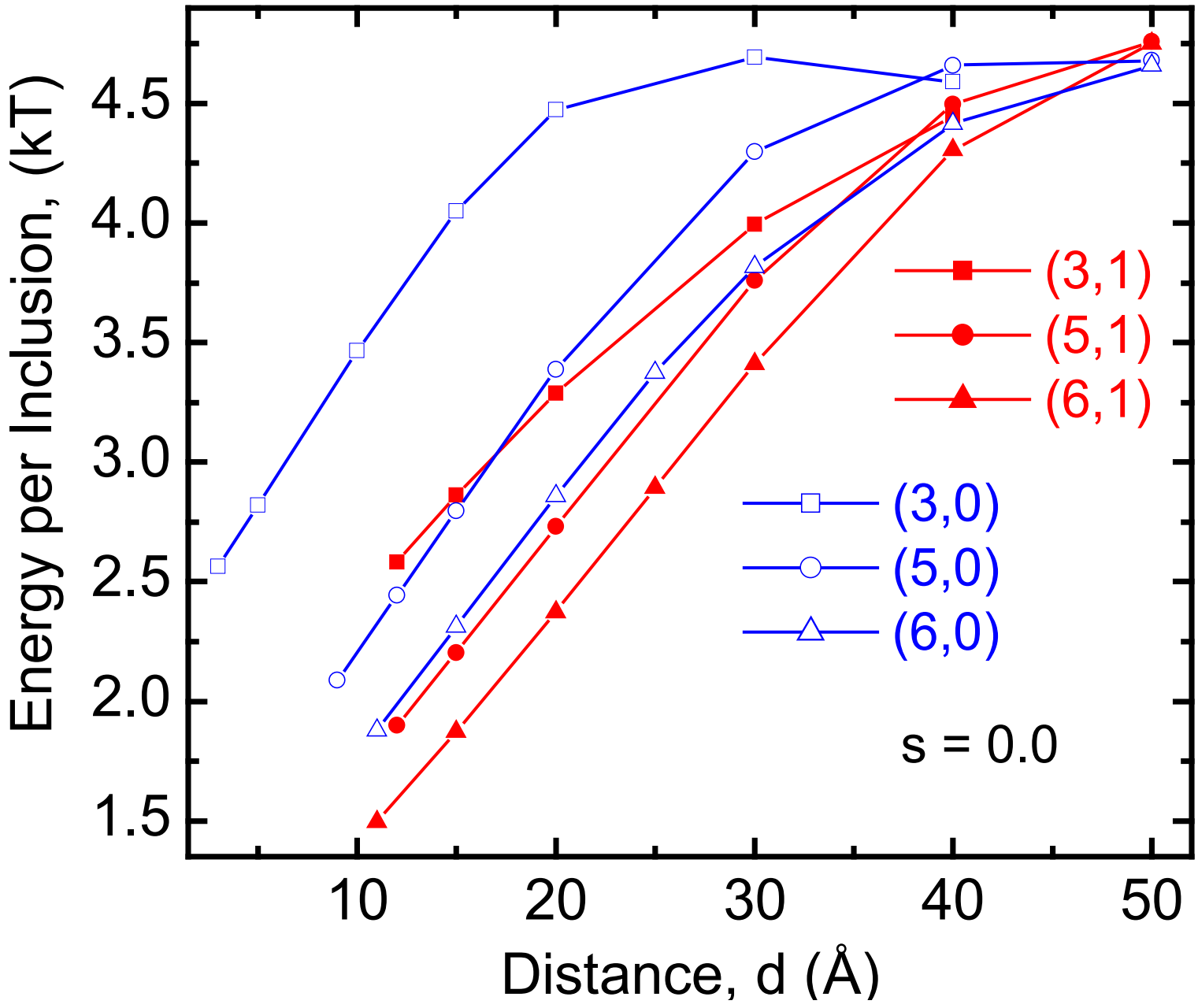

Fig. 7 Free energy of membrane deformation per inclusion as a function of distance, d, for s=0. Results are compared for clusters with (m=1) and without (m=0) a central inclusion.

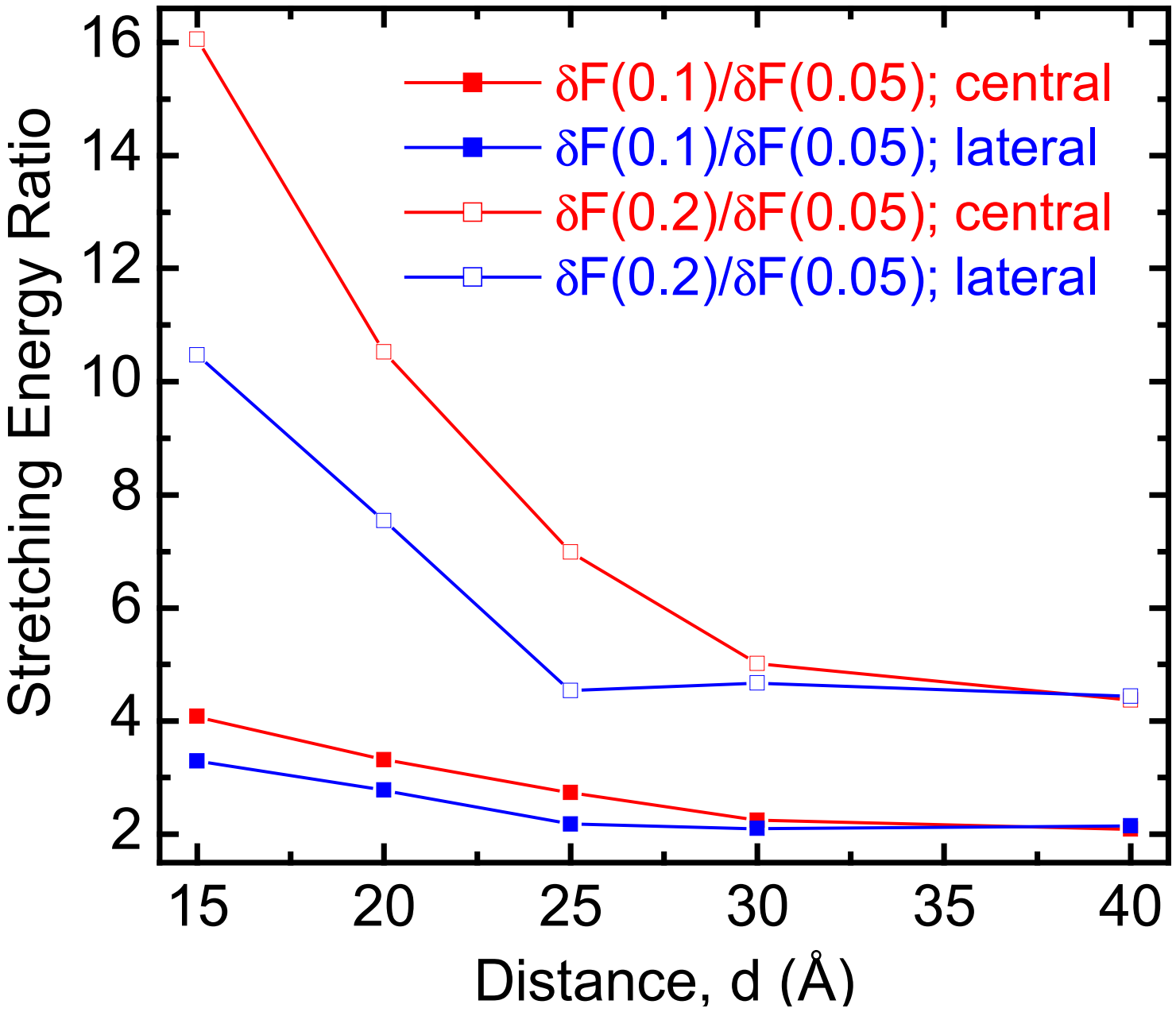

Fig. 8 Ratio of stretching energy for central and lateral inclusions in the (6,1) cluster as a function of d. Results are shown for the boundary slope s=0. Values of δu_0 *(in* Å) are given as the argument of the stretching energy δF.

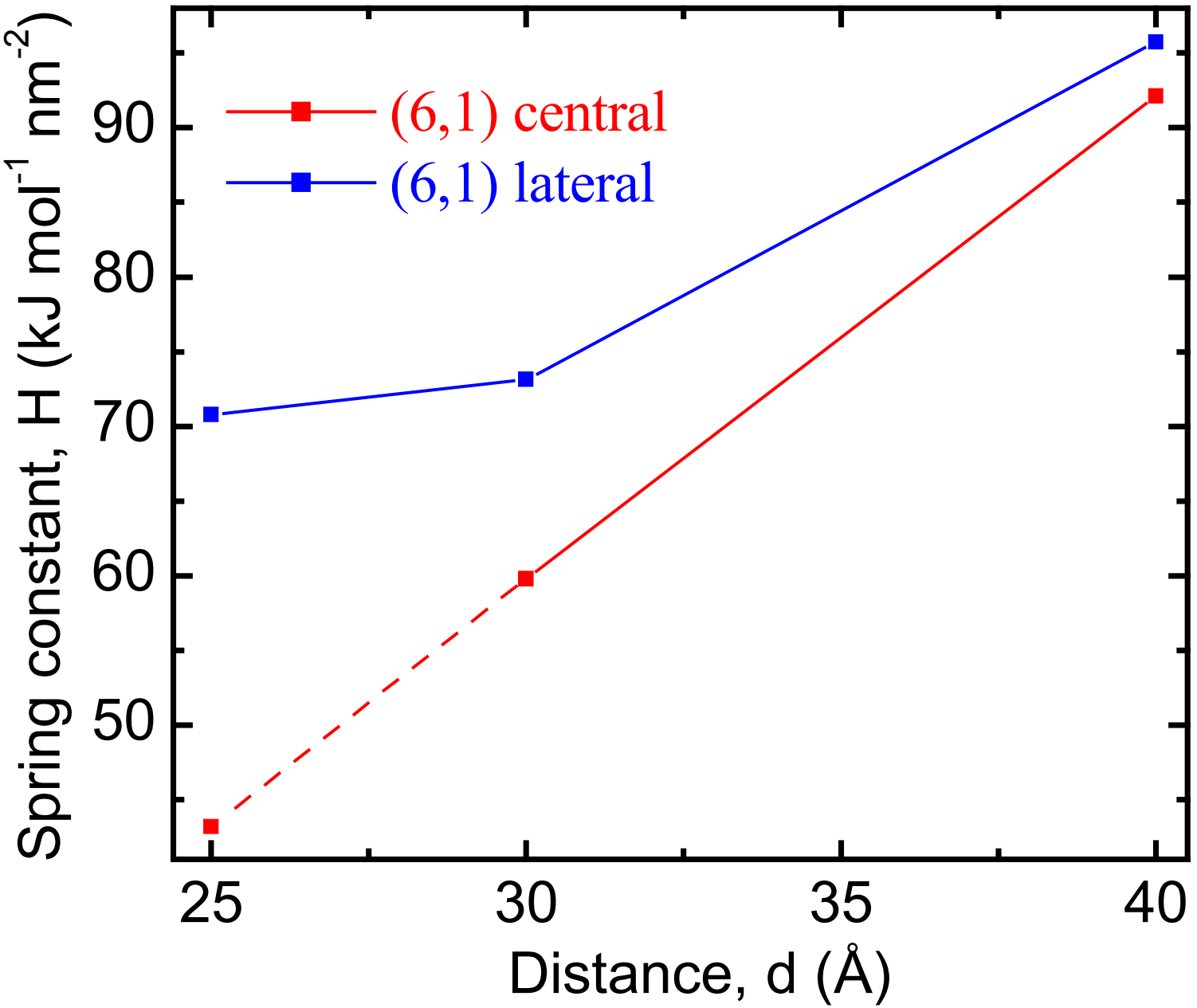

Fig. 9 Effective elastic constant, H, as a function of d for central and lateral insertions in a (6,1) cluster. Solid lines correspond to d ranges where Eqs. 4 & 5 apply (the dashed line is for d values slightly outside this range).